Zoological Studies **64:**27 (2025)

Visitors Without Passports: A Synthesis of Invasion Routes and Phylogeographic Patterns in the Asian Tiger Mosquito Based on Single-Locus Genetic Analyses

Juan C. Londoño-Sanchez[1,2], Carol E. Florez-Estrada[1,2], Bryan S. Valencia-Marin[1,3], and Oscar Alexander Aguirre-Obando[1,2,*]

[1]*Escuela de investigación en Biomatemática, Universidad del Quindío. Carrera 15, Calle 12 Norte, Armenia, Quindío, Colombia. *Correspondence: E-mail: oscaraguirre@uniquindio.edu.co (Aguirre-Obando)*
E-mail: juanc.londonos@uqvirtual.edu.co (Londoño-Sanchez); carole.floreze@uqvirtual.edu.co (Florez-Estrada); bsvalenciam@uqvirtual.edu.co (Valencia-Marin)

[2]*Programa de Biología, Universidad del Quindío. Carrera 15, Calle 12 Norte, Armenia, Quindío, Colombia*

[3]*Laboratorio de Fisiologia e Morfologia de Culicidae e Chironomidae, Universidade Federal do Paraná, Brasil*

(Received 24 January 2024 / Accepted 15 May 2025 / Published -- 2025)
Communicated by Chi-Chien Kuo

ORCiD:
Juan Camilo Londoño-Sanchez: https://orcid.org/0009-0001-3717-8852
Carol Estefani Florez-Estrada: https://orcid.org/0009-0009-6384-9638
Bryan S. Valencia-Marin: https://orcid.org/0000-0002-7844-4563
Oscar Alexander Aguirre-Obando:https://orcid.org/0000-0003-2480-7004

Aedes albopictus, a vector of arboviruses of medical and veterinary importance, has undergone a remarkable global expansion over the past five decades. This worldwide study analyzes the phylogeography, invasion routes, and demographic history of this mosquito species, tracing its spread from its native range in Asia to Oceania, Europe, America, and Africa. To this end, genetic datasets with distribution patterns aligned with the species' global spread were identified and extracted from publicly available databases. Phylogeographic analyses were conducted at a global level, invasion scenarios were tested, and the demographic history of populations involved in the spread was reconstructed. The mitochondrial genes *COI* (n = 3896), *ND5* (n = 597), and the complete mitogenome (n = 79) were analyzed, revealing higher genetic diversity within the native range and genetic connectivity across all invaded regions, including the Americas, Africa, Europe, and Asia. All genetic markers indicate that the invasion dynamics followed a panmictic population structure, characterized by random mating and high gene flow among populations. Demographic analyses confirm Asia as the ancestral source population and identify multiple introduction events into Europe, the Americas, and Africa. This invasion pattern, combined with the evidence of panmixia, suggests that anthropogenic factors—particularly global trade—play a pivotal role in

shaping the genetic connectivity and dispersal of *A. albopictus*, underscoring the influence of increasing global commerce on the spread of medically and veterinary-relevant species.

Keywords: *Aedes albopictus*, Demographic history, Gene flow, Maritime trade, Population genetics, *Stegomyia albopictus*

Citation: Londoño-Sanchez JC, Florez-Estrada CE, Valencia-Marin BS, Aguirre-Obando OA. 2025. Visitors Without Passports: A Synthesis of Invasion Routes and Phylogeographic Patterns in the Asian Tiger Mosquito Based on Single-Locus Genetic Analyses. Zool Stud **64:**27.

BACKGROUND

The tiger mosquito, *Aedes* (*Stegomyia*) *albopictus* (Skuse, 1894) (Diptera: Culicidae), is a vector of dengue, Zika, and chikungunya, and has demonstrated vector competence for an additional 32 arboviruses (Bonizzoni et al. 2013; Magalhaes et al. 2018; Näslund et al. 2021). While males feed primarily on flower nectar, females exhibit a preference for mammalian blood, including that of humans, although they may also feed on the blood of birds, amphibians, and reptiles to a lesser extent (Fikrig and Harrington 2021). Each female deposits up to 65 eggs during each oviposition event in a variety of environments—ranging from wooded areas to semi-urban and urban settings—employing both natural containers (*e.g.*, tree cavities, bamboo, bromeliads) and artificial containers (*e.g.*, tires, beverage containers) (Anoopkumar et al. 2017). Under optimal temperature conditions (25–30°C) and pH levels (5.2–7.6), the life cycle, from egg to adult, is completed within six to nine days. However, temperatures below 15°C or above 36°C disrupt the mosquito's life cycle (Waldock et al. 2013).

The tiger mosquito, *A. albopictus*, is native to Southeast Asia and has invaded tropical and subtropical regions across all continents over the past five decades, with the exception of Antarctica (Bonizzoni et al. 2013; Kraemer et al. 2015; Oliveira et al. 2021). The invasion process has been well-documented through historical records, which highlight its spread from Asia to other continents (Aguirre-Obando and Navarro-Silva 2017; Benelli et al. 2020). The first recorded instance of its presence outside its native range appears to have occurred in Europe, specifically in Albania (Adhami and Murati 1987). However, these early data do not provide information on the genetic connections between the native range and invaded regions, nor do they offer insights into potential invasion routes (Fischer et al. 2015).

Phylogeographic analyses, supported by genotypic data, have emerged as a valuable approach for understanding the invasion routes of disease vectors (Fontaine et al. 2021; Mallez et

al. 2018). In the case of the tiger mosquito, several phylogeographic studies have employed mitochondrial markers at the global level (mitogenome; Battaglia et al. 2016 2022), at the continental level (*COI* and *ND5* genes (Porretta et al. 2012), and at specific country levels (mitogenome, *COI*, and *Cytb* (Ibáñez-Justicia et al. 2022; Wibowo 2021)). These studies suggest a certain degree of gene flow between the invaded regions and Asia.

By employing Bayesian computational statistical methods, such as approximate Bayesian computation (ABC), alternative scenarios of demographic history can be evaluated, allowing the identification of the most plausible ones (Cornuet et al. 2014). Vega-Rúa et al. (2020) evaluated 71 demographic history scenarios for *A. albopictus* across 25 populations, identifying Asia—particularly East Asia (China)—as the native region. The invasion into Europe (Mediterranean Basin) and Africa (Réunion Island) was followed by a re-invasion into Europe (Italy). Populations originating from Asia (Japan) were introduced to America (initially the U.S. and subsequently to Mexico) before spreading to South America (Brazil). Central America was invaded by a combination of populations from South America (Brazil) and North America (U.S.). Populations of *A. albopictus* in Central Africa were traced back to an invasion event originating from South America (Brazil).

Although multilocus markers provide high resolution for genetic analyses, a single or a few molecular markers can also offer strong support to test genetic and/or gene flow hypotheses (Beerli and Palczewski 2010). In the context of population genetics, multilocus markers are ideal; however, their availability in genetic databases remains limited. In contrast, single-locus or few-locus markers offer lower genetic resolution but are more readily available in genetic databases. Therefore, the use of such markers at the population level would allow for the support, analysis, and assessment of hypotheses regarding migration processes, demographic history, routes of gene flow, and colonization of various medically important species (Athrey et al. 2012; Peretolchina et al. 2018; Ditter et al. 2022).

In this context, genetic databases play a crucial role in ensuring the availability and accessibility of genetic information for specific species. In the case of *A. albopictus*, a quick search in the BOLDSystem and GenBank repositories reveals the availability of 4,224 and 297,304 genetic sequences, respectively. This provides an opportunity to use available genetic data to evaluate population traits that support hypotheses regarding invasion routes, colonization dynamics, gene flow, and demographic history—areas that remain largely unexplored. Therefore, our work aims to address this gap by inferring the phylogeography, invasion routes, and demographic history of *A. albopictus* from its native range to other parts of the world, using genetic sequences available in databases.

MATERIALS AND METHODS

Search and selection of occurrences and genetic data

A comprehensive search for genetic sequences of *A. albopictus*, encompassing both nuclear and mitochondrial genomes, was conducted in the GenBank and BoldSystems databases. In GenBank, the search employed the species name, "*Aedes albopictus*," combined with the boolean operator AND and the specific genetic data to be retrieved, whether the complete genome or mitochondrial genes. Additionally, the boolean operator OR was used, followed by the abbreviations of the corresponding genes (Table S1). For the nuclear genome, complete genomes sequences were retrieved instead of individual genes, due to the large number of nuclear genes contained within the genome. For the mitochondrial genome, a search was conducted for 11 out of the 13 coding genes (Table S1), as these are commonly used in mosquito phylogeographic studies (Hasan et al. 2009; Moore et al. 2013; Morgan et al. 2011; Porretta et al. 2012).

For the BoldSystems database, only the species name and its synonyms were used, as this database primarily provides results for the Cytochrome C–Oxidase 1 (*COI*) gene. All searches included the synonyms associated with *A. albopictus*: *Culex albopictus, Stegomyia albopicta*, *Stegomyia samarensis*, *Stegomyia nigritia* and *Stegomyia quasinigritia*. Genetic data with georeferencing information exhibiting over 98% similarity with the species, according to BLAST analysis, was selected. This data was then mapped using QGIS v16.6 (QGIS, 2024). For this purpose, we used genetic markers from samples geographically distributed according to the species' natural range. The map was constructed using data collected up to 2014 from Kraemer et al. (2015) and supplemented with data through 2022 from the Global Biodiversity Information Facility (GBIF), with duplicate data removed in the final dataset.

The selected genetic data from the respective databases was downloaded, and renamed according to the country of origin. Alignment and trimming were performed using MAFFT v7 software (Katoh et al. 2018). The sequences were then analyzed to identify the presence or absence of pseudogenes (NUMTs), visualizing stop codons in the amino acid translations obtained in MEGA. From NUMT-free sequences, haplotypes (H) were identified, quantified, and ranked from highest to lowest frequency.

Phylogeographic analyses

Haplotype networks were constructed in R software version 3.5.1 using the Pegas package (Paradis 2010) and the haplonet function, based on the probability of parsimony criterion (Templeton et al. 1992). The resulting networks were graphically refined in Inkscape (www.inkscape.org). A single representative was selected for each haplotype, and the optimal model of nucleotide substitution was identified using the JmodelTest (Posada 2008). Based on this model, two phylogenetic trees were generated: one using maximum likelihood (ML) methods (RAXML v2.0.7 or MEGA v11.0.13) and the other using Bayesian inference (BI; BEAST v2.7.4). *Aedes aegypti* (GenBank accession number: MF194022) was used as the outgroup, from which the same gene regions analyzed in *A. albopictus* were extracted from the complete mitochondrial genome. The ML analysis was performed with 10,000 bootstrap replicates, and phylogenetic clusters were considered supported at bootstrap values ≥ 50. The BI analysis was run with 20 million generations, with clusters considered reliable at posterior probability values ≥ 0.9. To ensure the robustness of Bayesian inference, Markov chain mixing and effective sample size (ESS) were evaluated in Tracer v1.7.2, with parameter values required to reach ESS values ≥ 200 to be deemed robust. The resulting phylogenetic trees were visualized using Figtree and subsequently edited in Inkscape.

Migration scenarios

In addition, with the retrieved genetic information, assessment of various invasion scenarios and the demographic history of populations was carried out. Nine global invasion scenarios were considered (Fig. 1), selected to reflect key historical, commercial, and genetic connectivity factors influencing global dispersal. These included a panmictic model (panmixia; Fig. 1A), a full migration model (Fig. 1B), and several variations of stepping-stone models: two based on historical records (Fig. 1C–D), two reflecting intercontinental maritime trade routes (Fig. 1E–F), and three derived from the genetic connections revealed by the haplotype network (Fig. 1G–I).

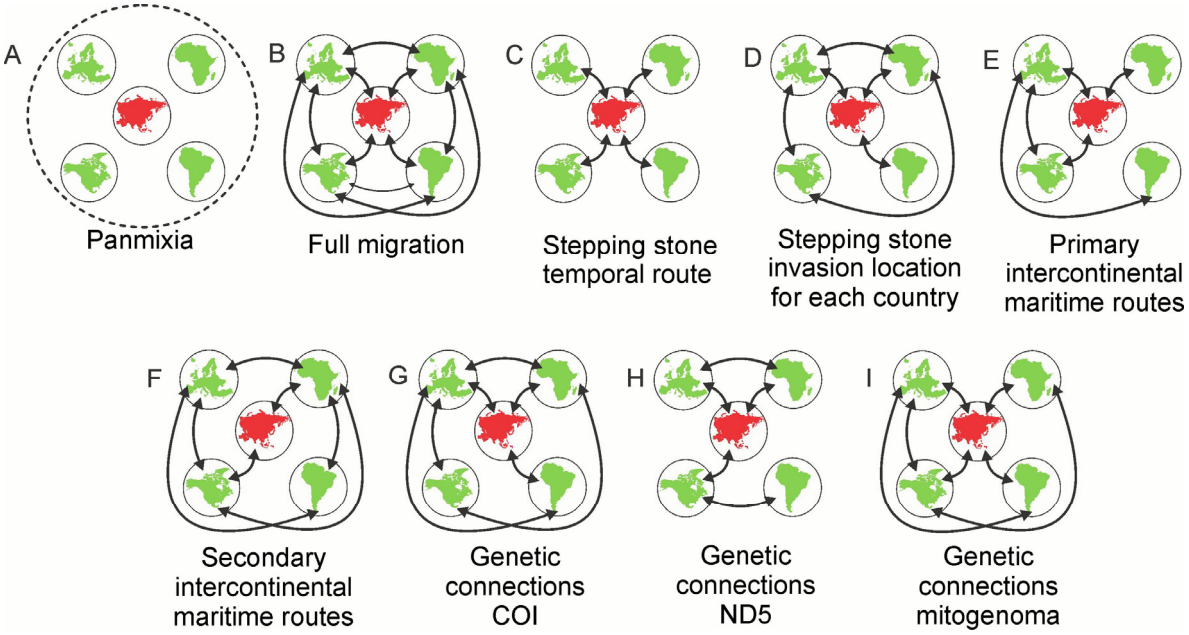

Fig. 1. Global gene flow scenarios for the Asian tiger mosquito. The red-colored population represents the native range in Asia, while green circles represent populations in invaded areas. The scenarios correspond to different migration hypotheses: (A) panmixia; (B) full migration; (C) stepping-stone model reflecting temporal routes; (D) invasion locations for each country; (E) primary intercontinental maritime routes; (F) secondary intercontinental maritime routes; and genetic connections inferred from haplotype networks for *COI* (G), *ND5* (H), and the mitochondrial genome (I).

The panmictic model represents a hypothesis of high and continuous gene flow among all sites ($Nm > 1$), in which all locations behave as a single population exhibiting random mating. In contrast, the full migration model assumes direct gene flow between all populations, with each remaining genetically distinct. Stepping-stone models restrict gene flow to spatially adjacent populations, relying on passive transport along networks—maritime in this case—to facilitate migration. Two historical stepping-stone models were developed based on the first documented records of the species in each country. The first follows a directional route based on the chronological order of appearance, while the second reconstructs the presumed source of invasion for each locality. To inform these historical models, we updated the global first-record dataset for *A. albopictus* from Aguirre-Obando and Navarro-Silva (2017) through a systematic search in Scopus and Google Scholar. Search terms included the species name followed by the Boolean connector OR with its synonyms, and then AND with the keyword "*first record*" and the country name. Searches were conducted in both English and Spanish. The first scenario considered primary trade routes supporting large-scale commercial shipping to major markets, while the second included secondary routes linking smaller markets. Route information was obtained from Rodrigue (2020). All models were evaluated using the coalescence-based program Migrate-N v5.0.4 (Beerli and Palczewski 2010; Beerli et al. 2019) and were run online via the CIPRES Science Gateway platform.

To assess migration patterns, two complementary approaches were implemented using haplotype data, in accordance with prior recommendations emphasizing the importance of homogenizing genetic datasets across populations and mitigating biases caused by unequal sample sizes (Kotsakiozi et al. 2011; Neophytou 2013; Frost et al. 2015; Puechmaille 2016). Disproportionate sampling can artificially inflate migration estimates in overrepresented populations, thereby skewing interpretations of gene flow patterns.

The first approach used a homogeneous dataset, in which all populations were standardized to the smallest haplotype count. This was achieved by randomly selecting sequences in R, ensuring unbiased haplotype representation across populations (Wang, 2016; Magee et al. 2017; Vavassori et al. 2022). The second approach employed a heterogeneous dataset, retaining the natural distribution and abundance of haplotypes observed in each population. In both approaches, a single representative sequence per haplotype was included to ensure analytical consistency and comparability (Sherpa et al. 2018; Pichler et al. 2019).

Although homogeneous datasets are generally favored in the literature, both datasets were analyzed to evaluate the consistency of results across methodological frameworks. This approach aligns with multiscenario validation protocols that emphasize ecological variability and statistical rigor (Baele et al. 2017; Rasmussen, 2021; Vavassori et al. 2022).

Demographic history analysis

To infer the demographic history of *A. albopictus*, various invasion scenarios were evaluated using DIY-ABC v2.0 (2014) (Cornuet et al. 2014). Due to the complexity and the number of possible evolutionary routes, a stepwise analytical strategy was adopted, focusing on macrogeographic subgroups, as in previous studies (Manni et al. 2017) and Vega-Rúa et al. 2020). Two main categories of scenarios were constructed: (1) single introduction, following the chronological order suggested by the first historical records (Fig. 2) and (2), split introduction considering multiple independent invasions in newly colonized regions. Additionally, models from previous literature—Admixture, No Admixture, and Admixture vs. No Admixture—were also tested (Manni et al. 2017; Maynard et al. 2017; Sherpa et al. 2019; Vega-Rúa et al. 2020). Scenario construction incorporated key demographic parameters, including mixing levels, bottleneck effects, and estimated invasion times (expressed in generations). Generational estimates were based on 12 generations per year for tropical regions and 7 for subtropical ones. When such information was lacking—especially for native populations—uniform priors [10–100,000] were applied (Cornuet et al. 2014). Genetic evidence guided the selection of countries included in the analyses. These countries were initially categorized based on their latitudinal distribution into tropical and

subtropical/temperate zones (Fig. 3). Generational time was then estimated from the year of the first recorded invasion up to 2022 (Table S2), assuming 12 generations per year for tropical countries and 7 generations per year for subtropical and temperate countries, following prior demographic analyses of *A. albopictus* conducted using approximate Bayesian computation (Manni et al. 2017; Maynard et al. 2017; Sherpa et al. 2019; Vega-Rúa et al. 2020). In instances where the invasion records were unavailable, such as in the native range, uniform priors [10–100.000] were deliberately applied (Cornuet et al. 2014). Analyses were conducted over 10 million generations, with all scenarios compared using posterior probability (PP) tests implemented within a logistic regression framework, incorporating 1% of the dataset and retaining a single intermediate value. Additionally, a confidence test was performed across all evaluated scenarios using 1% of the dataset in logistic regression. Upon identifying the most probable scenario, it was re-evaluated under the assumption that all populations experienced bottleneck events. The best-supported scenario for each continent was subsequently integrated to construct a global model representing the invasion history of*A. albopictus*.

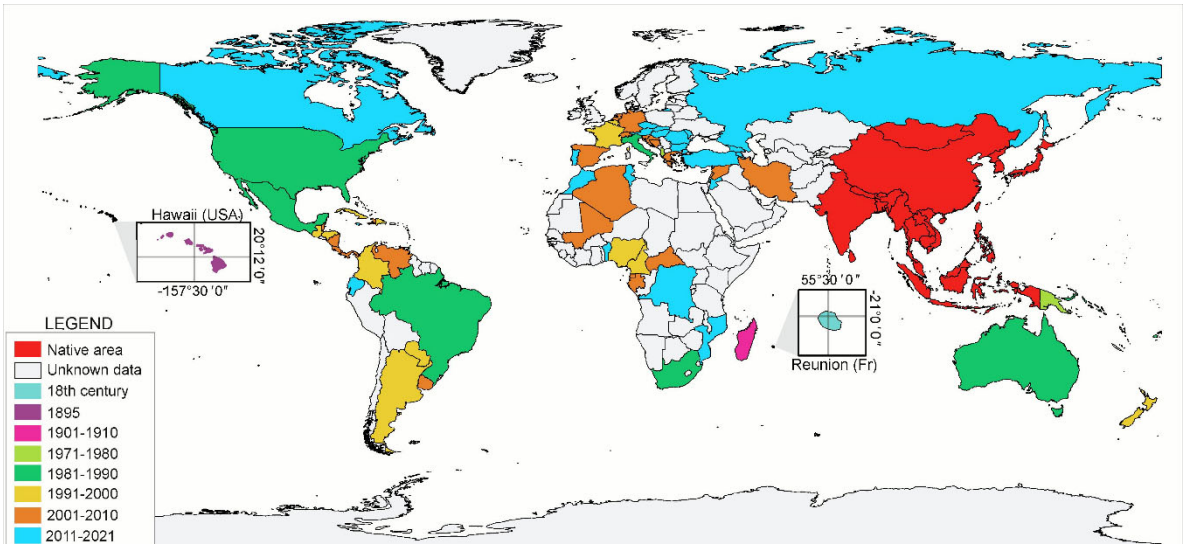

Fig. 2. First recorded invasions of the tiger mosquito worldwide, displayed by decade according to the color scale shown in the legend.

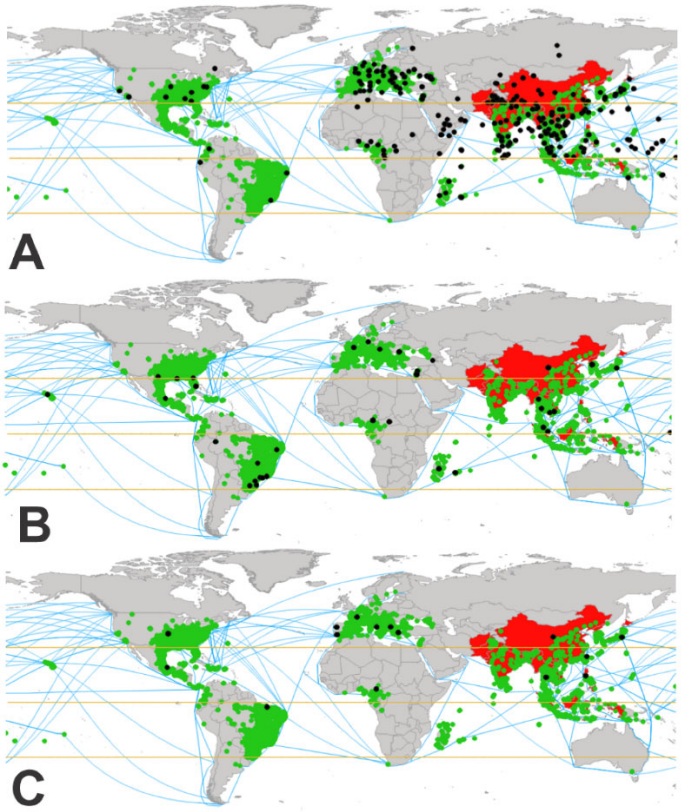

Fig. 3. Geographic distribution of occurrences (green dots) and genetic records (black dots) of *A. albopictus*, including its native range (red) and major maritime trade routes (blue lines). Maps are organized by the frequency of available genetic information, from highest to lowest: *COI* (A), *ND5* (B), and mitochondrial genome (C).

Classical tests of genetic diversity, neutrality tests, and genetic structuring

At the global, continental, and national scales, classical measures of haplotype diversity and Tajima's D neutrality test (Tajima 1989; Tajima et al. 1998) were computed using the RStudio environment with the 'pegas' package (Paradis 2010). Additionally, analyses of molecular variance (AMOVA) were conducted to assess genetic structuring at the continental level, by country, and among countries. Furthermore, pairwise FST tests were performed to evaluate genetic differentiation between continents and among countries.

RESULTS

A total of 21,593 occurrence records for *A. albopictus* were compiled up to 2022, with 37.64% sourced from Kraemer et al. (2015) and 62.36% updated from GBIF. These records document the species' presence across nearly every continent—except Antarctica—and its distribution across tropical (34.78%) and subtropical (65.22%) regions. The genetic data, mirroring the species' distribution, included mitochondrial DNA (mtDNA) sequences for *COI* (n = 4,234),

ND5 (*n* = 524), and complete mitochondrial genomes (n = 84). In contrast, nuclear genome data (n = 77) and mitochondrial genes *Cytb* (*n* = 17), *COII* (*n* = 8), *ND4* (*n* = 7), and *ND3* (*n* = 3) did not meet the selection criteria and were excluded from analyses. Data for other mitochondrial genes were either unavailable or not retrieved.

After alignment and trimming, the mtDNA *COI* gene fragment (300 bp; *n* = 3,896) was distributed across 71 countries and six continents, with the highest representation in Asia (57.29%; 22 countries), followed by Europe (13.27%; 17 countries), Oceania (12.68%; 6 countries), North America (6.42%; 4 countries), Africa (3.26%; 7 countries), and South America (2.08%; 3 countries). Genetic data for the mtDNA *ND5* gene and the mitochondrial genome were available for five continents. The mtDNA *ND5* gene (236 bp; (*n* = 597) was distributed across 29 countries and two islands, with a notable presence in Asia (70.69%, 12 countries), followed by Africa (14.57%, 3 countries), Europe (7.54%, 10 countries), North America (4.19%, 2 countries), and South America (3.02%, 2 countries). The mitochondrial genome (14,580 bp; *n* = 79), was recorded in 8 countries, with the majority of data originating from Europe (41.78%; 2 countries), followed by Asia (29.11%; 3 countries), North America (14.29%; 1 country), South America (6.49%; 1 country), and Africa (5.10%; 1 country).

Table 1 presents the results for haplotype diversity (Hd), nucleotide diversity (π), and Tajima's neutrality tests (D) at the global and continental scales, while table S3 provides these metrics at the country level. Across global, continental, and national datasets, haplotype diversity was consistently higher for the *COI* and *ND5* genes (Hd = 0.613–1.000) than for the complete mitochondrial genome (Hd = 0.000–0.004). Nucleotide diversity for the mitochondrial genome was generally greater at the continental level (π = 0.865–0.978) than at the country level (π = 0.400–1.000). In contrast, nucleotide diversity for the *COI* and *ND5* genes was consistently lower than that observed for the mitochondrial genome, regardless of the geographical scale. Tajima's D values varied across continents and countries, with both negative and positive values recorded, consistent with the test's assumptions regarding neutrality.

Table 1. Global and continental -level analyses for the *COI*, *ND5*, and mitochondrial genome of the tiger mosquito. The results include estimates of haplotype diversity (Hd) nucleotide (π) diversity, and neutrality tests outcomes

Geographic scale	Genetic diversity						Neutrality test		
	Hd			π			Tajima's D		
	COI	*ND5*	Mitogenome	*COI*	*ND5*	Mitogenome	*COI*	*ND5*	Mitogenome
Global	0.795	0.257	0.98	0.007	0.005	0.002	-2.445*	-2.545*	-2.815*
Africa	0.513	0.132	0.667	0.002	0.001	0.001	-1.500	-1.044	2.264*
Asia	0.798	0.243	0.978	0.012	0.006	0.004	-2.291*	-2.522*	-1.842
Europe	0.363	0.130	0.945	0.001	0.001	0.001	-2.676*	-1.871*	-1.675
America	0.452	0.578	0.865	0.003	0.003	0.001	-2.435*	-1.280	-3.531*
North America	0.216	0.230	N/A	0.002	0.001	N/A	-2.683*	-1.886	-2.556*
South America	0.663	0.307	N/A	0.004	0.001	N/A	1.452	-1,096	N/A
Islands in the Indian Ocean (Africa)	0.353	N/A	N/A	0.001	N/A	N/A	-1.065	N/A	N/A
Oceania	0.774	N/A	N/A	0.006	N/A	N/A	-0.794	N/A	N/A

*Significant values ($p < 0.05$); N/A values not recorded.

AMOVA analyses revealed population structure at the continental level for the *COI* gene, and among countries within continents and between countries for all three mitochondrial markers (Table 2). The FST fixation index indicated significant genetic structuring at both continental and inter-country levels for all markers (Fig. 4).

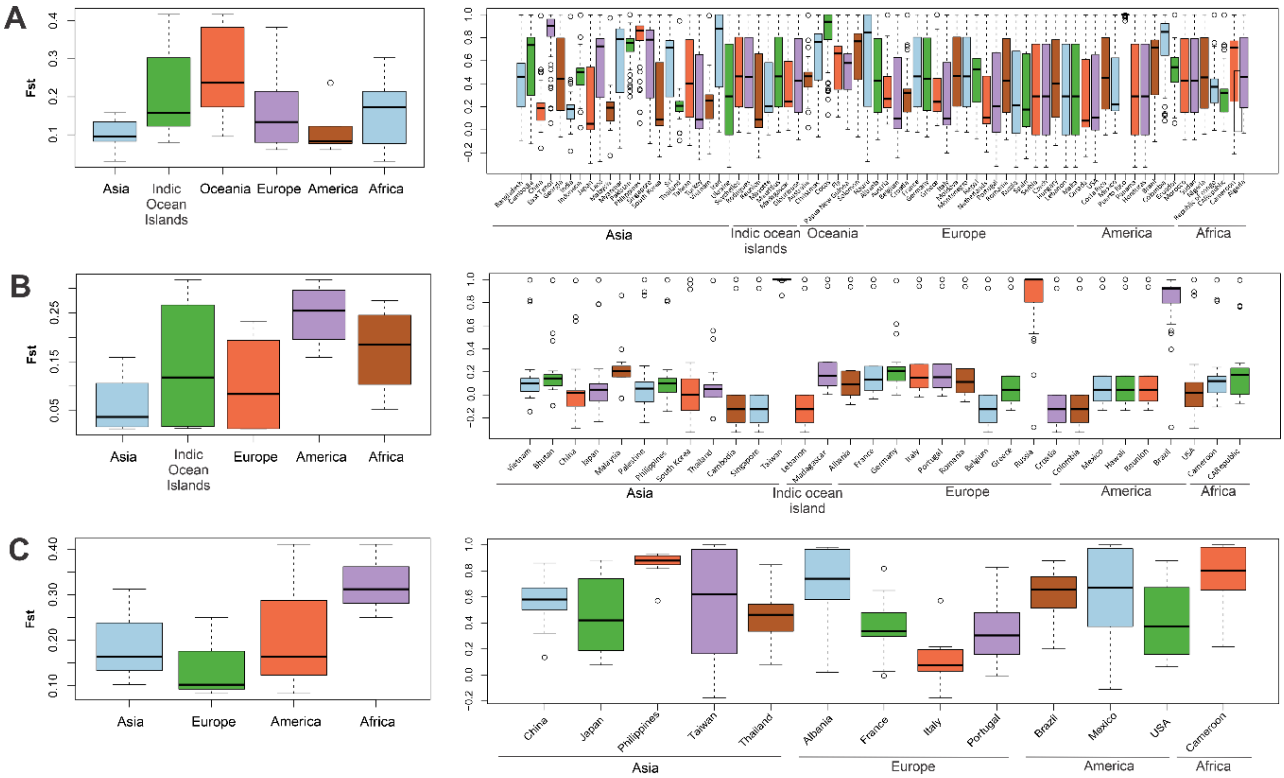

Fig. 4. Boxplots for the FST fixation index at the continental level (left) and country level (right) for the genes *COI* (A), *ND5* (B), and mitogenome (C).

Table 2. Continental- and country-level results for tiger mosquito populations, along with AMOVA analyses for the *COI*, *ND5*, and mitochondrial genome markers

	d.f.			Percentage of variation			*p*-value		
Source of variation	*COI*	*ND5*	Mitogenome	*COI*	*ND5*	Mitogenome	*COI*	*ND5*	Mitogenome
Between continents	5	3	3	4.82	-18.15	-0.67	0.000***	0.475	0.301
Within countries within continents	68	28	10	21.34	50.82	28.64	0.000***	0.000***	0.001***
Between countries	3786	565	63	73.85	67.33	72.02	0.017*	0.000*	0.015*
Total	3859	596	76	100.00	100.00	100.00			

*Significant values ($p < 0.05$); ***Significant values ($p < 0.001$).

A total of 255 haplotypes were identified for the mitochondrial DNA (mtDNA) *COI* gene, with some haplotypes shared across continents and others unique to specific regions. The proportion of global haplotypes by continent was as follows: Asia (89.41%), Europe (11.37%), Oceania (6.27%), Africa (4.31%), and the Americas (3.53%). For the mtDNA *ND5* gene, 30 haplotypes were detected, distributed across four continents: Asia (86.7%), the Americas (20%), Oceania (13.3%) and Africa (10%). Likewise, for the mitochondrial genome, 48 haplotypes were recovered in four continents: Asia (35.3%), Europe (25.1%), the Americas (23%), and Africa (4.2%) (Fig. 5).

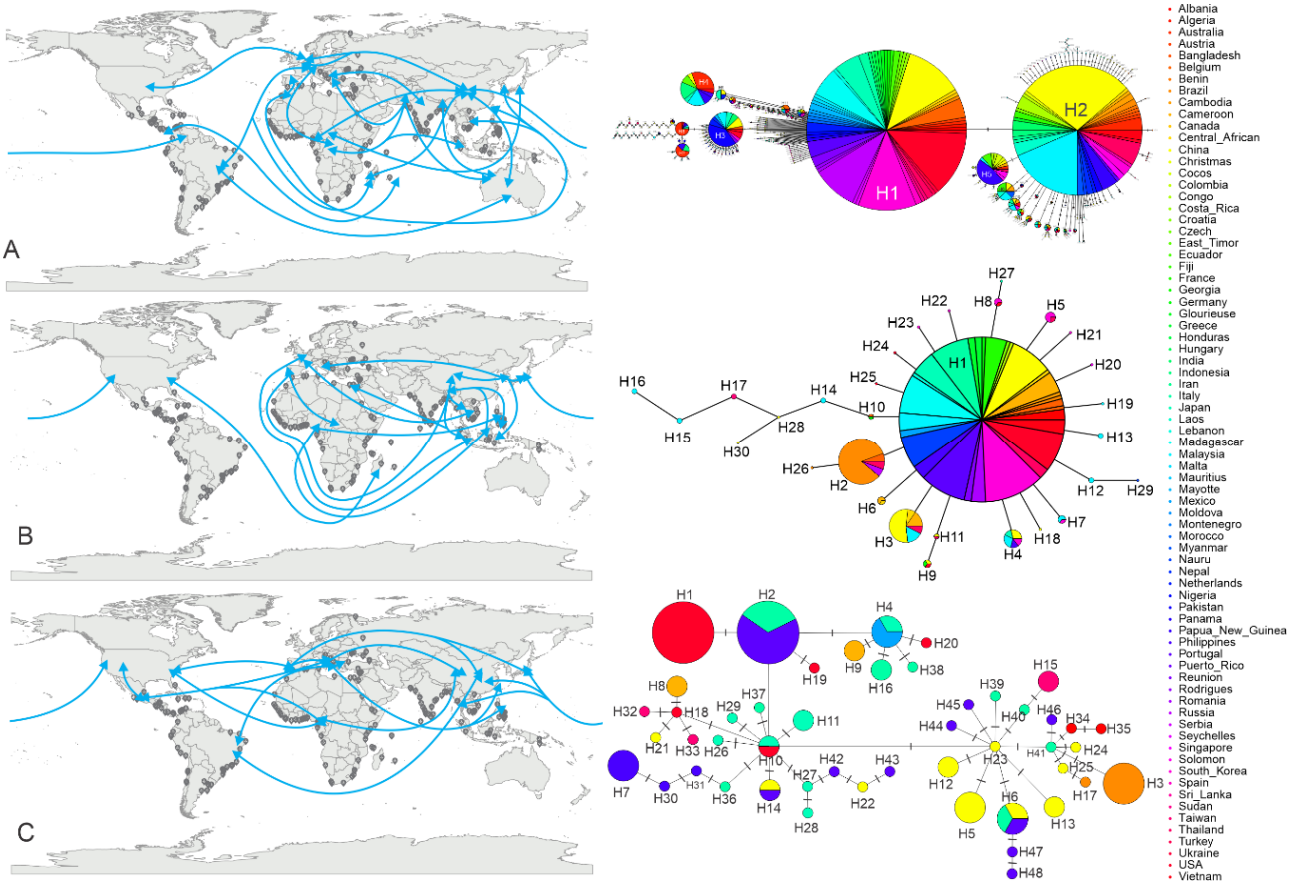

Fig. 5. Global genetic connections for mtDNA *COI* (A), *ND5* (B), and mitochondrial genome (C) of the tiger mosquito. Blue arrows (left column) represent inferred gene flow based on haplotype networks (right column), where circle size is proportional to haplotype frequency.

Figure 6 displays the phylogenetic trees constructed for the mitochondrial *COI* and *ND5* genes, as well as the complete mitochondrial genome, using both maximum likelihood (ML) and

Bayesian inference (BI) methods. Black circles denote nodes with bootstrap support ≥ 50 and posterior probability ≥ 90. The Markov chains in the BI analysis reached stationarity, and the effective sample size exceeded 200 for all parameters. Although comparable clades were retrieved across all datasets, differences in tree topology were evident. Clades based on complete mitochondrial genomes received strong statistical support (bootstrap ≥ 50%; posterior probability ≥ 70%), whereas those derived from partial gene regions failed to reach comparable levels of confidence. No clear geographic clustering was observed among the samples. Nonetheless, all mitochondrial clades included distinct haplotypes of Asian origin (highlighted in red in Fig. 6), underscoring their widespread phylogenetic distribution.

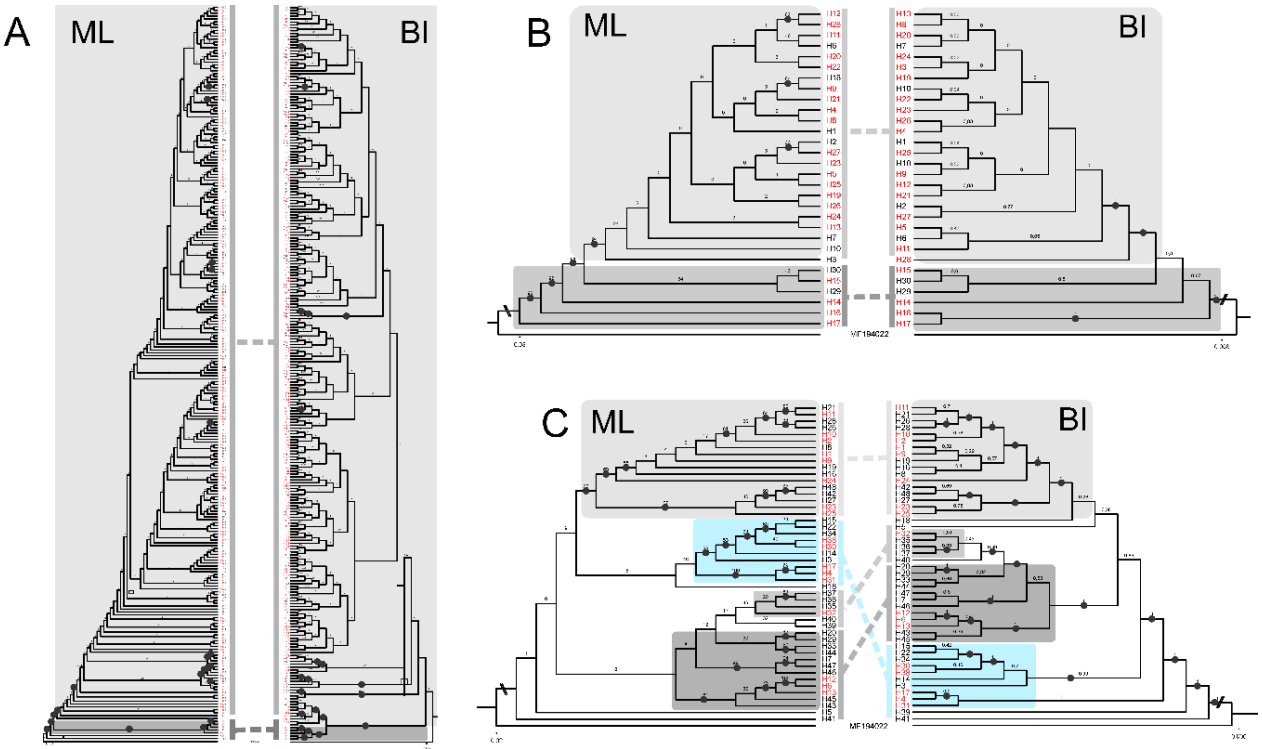

Fig. 6. Clustering trees constructed under maximum likelihood and Bayesian inference approaches for mitochondrial genes *COI* (A), *ND5* (B), and the mitochondrial genome (C). All analyses were run with 10,000 Bootstrap repetitions for ML and 20 million generations for BI, using nucleotide substitution models: GTR+I+G (*COI*), HYG+G (*ND5*), and GTR+G (mitogenome). Black circles indicate bootstrap support ≥ 50 and posterior probability ≥ 90. In the Bayesian inference analysis, the Markov chains were stabilized, and the effective sample size was greater than 200 for all parameters. Asian haplotypes are shown in red for each clade. Identical colors between clades denote similar clades, and the dashed arrows between them indicate their topological positioning.

For migration analyses, *COI* data encompassed six continents, whereas *ND5* and mitochondrial genome data were limited to five. To standardize populations numbers across markers, Oceania was excluded from the *COI* dataset, enabling a consistent comparative framework for testing migration hypotheses (Fig. 1). In these analyses, continents were treated as population units, each comprising all associated countries (Table S3). The homogeneous dataset included three haplotypes per population for *COI* and *ND5*, and two for the mitochondrial genome. In contrast, the

heterogeneous dataset incorporated all observed haplotypes per population. Haplotype distributions were as follows: *COI* (Asia: 223; Europe: 29; North America: 7; South America: 3; Africa: 6), *ND5* (Asia: 26; Europe: 4; North America: 4; South America: 3; Africa: 3), and mitochondrial genome (Asia: 22; Europe: 15; North America: 7; South America: 2; Africa: 2). Table 3 summarizes the results of the migration analysis, including marginal Bézier likelihood (lmL), logarithmic Bayes factor (LBF), posterior probability (PP), and scenario rankings. Collectively, the genetic evidence supports a panmictic population structure (Fig. 7).

Table 3. Marginal likelihood values based on Bézier approximation (lmL), logarithmic Bayes factor (LBF), posterior probability (PP), and scenario rankings for global migration patterns of the tiger mosquito were evaluated across populations using both heterogeneous and homogeneous datasets. The most plausible scenario for each marker is highlighted in gray. The best scenario was selected based on the highest posterior probability and the lowest LBF value

Heterogeneous N												
	lmL			LBF			PP			*Ranking*		
Scenario	*COI*	*ND5*	Mitogenome	*COI*	*ND5*	Mitogenome	*COI*	*ND5*	Mitogenome	*COI*	*ND5*	Mitogenome
Panmixia	-1136.56	-1042.8	-20817.13	0	0	0	1.00	1.00	1.00	1	1	1
Full migration	-1200.44	-1068.45	-21160.5	-127.76	-51.3	-686.74	0.00	0.00	0.00	4	2	2
SS H1	-1205.81	-1071.36	-21292.42	-138.5	-57.12	-950.58	0.00	0.00	0.00	6	3	4
SS H2	-1205.49	-1071.72	-21358.5	-137.86	-57.84	-1082.74	0.00	0.00	0.00	5	4	6
SS M1		-1072.59	-21348.69		-59.58	-1063.12	0.00	0.00	0.00		5	5
SS M2	-1143	-1073.9	-21509.43	-128.80	-62.2	-1384.6	0.00	0.00	0.00	2	7	7
SSGC	-1143.1	-1073.45	-21207.86	-130.79	-61.3	-781.46	0.00	0.00	0.00	3	6	3
Homogeneus N												
Panmixia	-499.85	-470.79	-17875.21	0	0	0	1.00	1.00	1.00	1	1	1
Full migration	-522.7	-491.4	-18000	-45.7	-41.22	-249.58	0.00	0.00	0.00	5	2	6
SS H1	-524.12	-495.74	-18014.65	-48.54	-49.9	-278.88	0.00	0.00	0.00	7	7	7
SS H2	-524.1	-493.37	-17961.83	-48.5	-45.16	-173.24	0.00	0.00	0.00	6	5	2
SS M1	-506.09	-492.84	-17970.89	-124.79	-44.1	-191.36	0.00	0.00	0.00	4	4	3
SS M2	-504.11	-492.62	-17981.55	-851.99	-43.66	-212.68	0.00	0.00	0.00	2.5	3	5
SSGC	-504.11	-494.57	-17981.1	-851.99	-47.56	-211.78	0.00	0.00	0.00	2.5	6	4

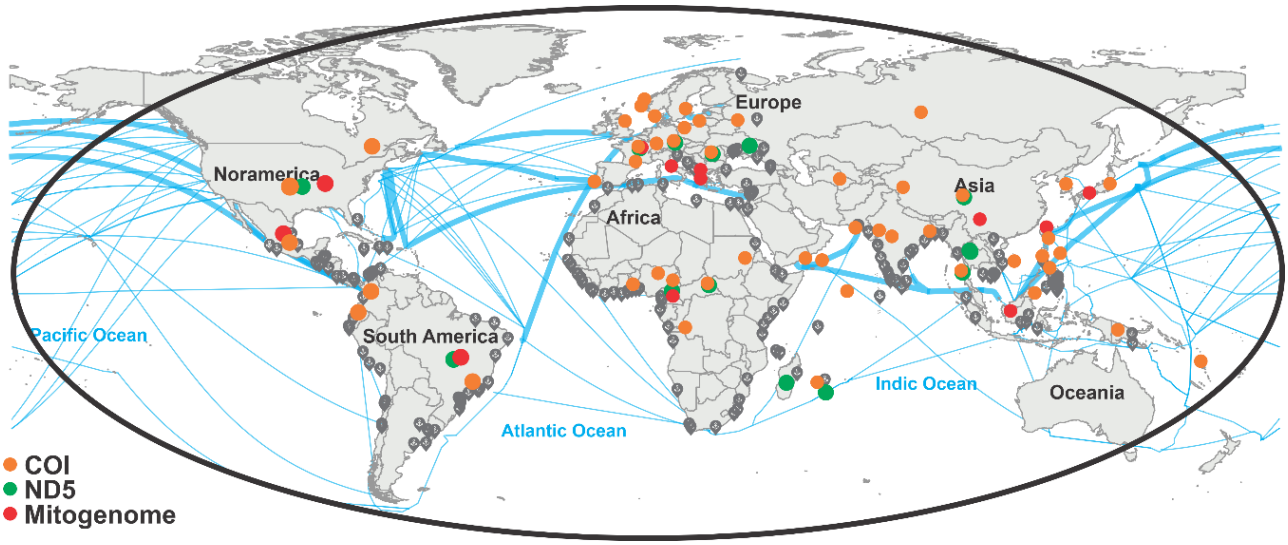

Fig. 7. Most probable migration scenarios for the *COI*, *ND5*, and mitochondrial genome genes. The names of the populations included in the analysis are shown. Blue lines represent primary and secondary intercontinental maritime transport routes, while gray points indicate the locations of primary and secondary maritime ports.

For demographic history analyses, the number of sequences was standardized based on the smallest sample size among countries, resulting in datasets comprising 63 countries (n = 189) for

the *COI* gene, 19 countries (n = 57) for the *ND5* gene, and 12 countries (n = 24) for the mitochondrial genome. A total of 138 demographic history scenarios were evaluated, distributed as follows: 60 scenarios for the *COI* gene (37 single introduction scenarios; 23 admixture scenarios), 40 scenarios for the *ND5* gene (25 single introduction; 15 admixture), and 38 for the mitochondrial genome (18 single introduction; 20 admixture).

All three genetic markers indicate that Southeast Asia is the native region of the mosquito, from which it has dispersed to the Indian Ocean islands (1716 and F3680 generations), Oceania (1971 and F614), Europe (1977 and F317), North America (1985 and F260), and Africa (1991 and F383). The suggested ancestral population at the continental level was consistent across markers, except for South America (Brazil), where the *COI* gene suggests a single introduction from China, the *ND5* gene indicates an origin from Réunion Island, and the mitochondrial genome supports an admixture event between U.S. and China. Table S5 presents the directional flow for each scenario, along with their posterior probabilities and the results of the confidence tests.

When the analyses were conducted at the continental scale, Asia was identified as the source region for all other continents. However, country-level analyses revealed that the initially invaded country within each continent harbored ancestral populations originating from different regions within Asia (Table S2 and Fig. 2). For Madagascar (Indian Ocean), mitochondrial haplotypes indicate an introduction from Southeast Asia, with the *COI* gene pointing to Indonesia and the *ND5* gene suggesting Thailand as the source population. In Albania (Europe), the mitochondrial genome and *COI* gene both suggest an ancestral origin in China, whereas the *ND5* gene points to Thailand. The introduction into Cameroon (Africa) is attributed to an ancestral population from Thailand according to the *COI* and *ND5* genes, while the mitochondrial genome supports a mixed origin involving Japan and China. Finally, the introduction to the U.S. (North America) was consistent across all three markers, each identifying China as the source of the ancestral population. All three mitochondrial markers also indicate that mosquito populations in Europe, the Americas, and Africa underwent genetic bottlenecks ranging from 11 to 47 generations (see Fig. 8).

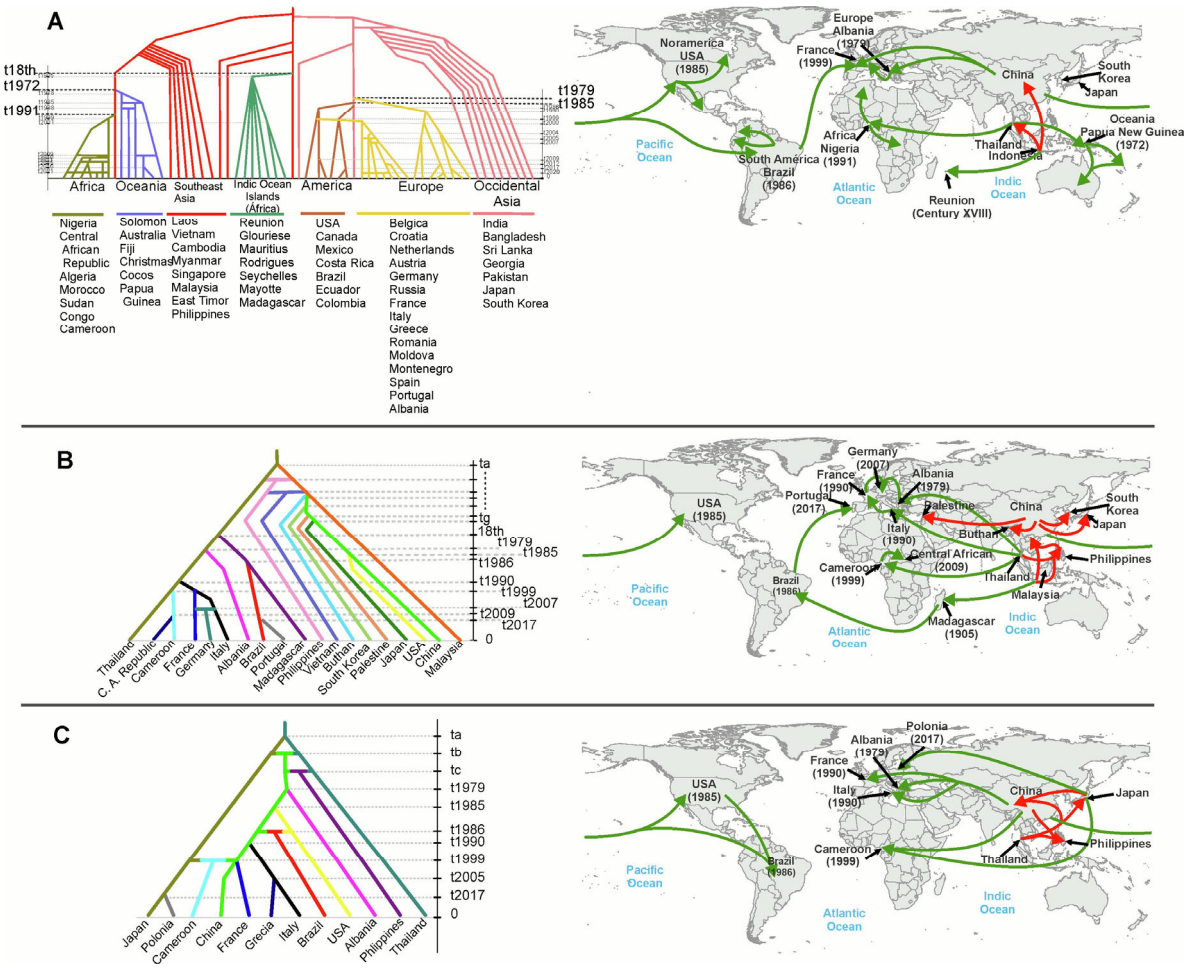

Fig. 8. Global demographic history scenarios for the Asian tiger mosquito inferred from the mtDNA *COI* gene (A), *ND5* gene (B), and mitochondrial genome (C). The scenario with the highest posterior probability is shown on the left, and its geographical representation is shown on the right. Red lines indicate the directionality of populations within the native range, while green arrows indicate the directionality of populations in invaded areas.

DISCUSSION

To the best of our knowledge, this study represents the first comprehensive synthesis of *A. albopictus* genetic data retrieved from public databases. We examined the species' population genetics, invasion dynamics, and demographic history across multiple geographic scales—global, continental, and national. Our results reveal that haplotype number, nucleotide diversity, and haplotypic diversity are highest in Asia, the species' native region, aligning with previous studies (Birungi and Munstermann 2002; Shin et al. 2023).

In general, species tend to exhibit greater genetic diversity in their native regions compared to introduced areas (Carter et al. 2010; Nadel et al. 2010; Boissin et al. 2012; Gotzek et al. 2015; Comeault et al. 2020). Invasive species often experience reductions in genetic diversity in non-native regions due to founder effects and demographic bottlenecks during colonization. These

processes lead to increased homozygosity of deleterious alleles, reduced heterozygosity-driven fitness advantages, and ultimately lower overall fitness. However, invasive species appear to overcome these constraints through high migration rates from their native ranges (Estoup 2016), a phenomenon also observed in other mosquito species (Becker et al. 2012; Estoup 2016).

Interestingly, the *ND5* gene revealed an unusually high haplotype diversity (Hd) in the Americas, despite this region not being part of the species' native distribution. One possible explanation is the high level of maritime connectivity between Asia and the Americas, given that 10 of the world's 25 busiest seaports are located along these intercontinental trade routes. This high level of connectivity may indicate substantial gene flow facilitated by anthropogenic transport, particularly between Asia and the Americas (Carlton 1987; Hudson et al. 2022). Passive transportation mediated by human activities has played a crucial role in the long-distance spread of medically important mosquito species, especially through the movement of containers such as used tires—a well-documented pathway for *A. albopictus* (Elbers et al. 2015; Ibañez-Justicia et al. 2020). Frequent intercontinental connections, combined with the high genetic diversity of Asian populations, may lead to invaded populations retaining substantial genetic variability, a phenomenon known as polymorphism retention (Suesdek 2019).

Neutrality test results at global, continental, and national scales for the three mitochondrial markers revealed a mix of significant positive and negative values, indicating departures from neutrality (Porretta et al. 2012). Analyses of genetic diversity at continental and country scales yielded both negative and positive values in neutrality tests, including Tajima's D, reflecting diverse demographic and evolutionary dynamics among populations. Negative values may indicate positive selection, where advantageous variants increase in frequency, or signal ancient population expansion events associated with colonization or migration, followed by periods of stabilization or decline. Additionally, they may reflect population structure with geographical subdivisions or restrictions to gene flow between subpopulations. On the other hand, positive values may indicate a possible recent demographic expansion in the population or the action of purifying selection, removing harmful variants. Understanding these patterns provides valuable insights into the evolutionary processes shaping population dynamics and genetic diversity in *A. albopictus* (Tajima 1989; Láruson and Reed 2021).

In general, most populations at the continental and inter-country levels exhibited both negative and positive values in the neutrality test. Specifically, the *COI* gene showed that 73.2% of populations conformed to neutrality, a pattern similar to the 71.4% observed in populations analyzed with the *ND5* gene and the 50% observed in populations assessed using mitochondrial genome markers. These results are consistent with previous analyses based on *COI* mtDNA, which

also reported neutrality in most globally distributed populations (Zhong et al. 2013; Ruiling et al. 2018).

Across all three markers, over half of the evaluated populations yielded negative neutrality values, suggesting recent demographic expansion likely linked to bottlenecks. One potential cause could be the implementation of vector control measures using insecticides to manage epidemiological outbreaks of arbovirus transmission, reducing mosquito populations. However, once the insecticide is no longer applied, the remaining populations can rapidly expand (Ruiling et al. 2018).

AMOVA results at the continental level only indicated genetic structuring for the *COI* gene, whereas all three markers detected structure at the country level both within and across continents. The lack of genetic structuring observed for the *ND5* gene and the mitochondrial genome at the continental scale, compared to the *COI* gene, could be explained by two factors. First, it may reflect a high rate of migration and gene flow between continents (Latreille et al. 2019). Second, it could be associated with the lower number of sequences per locality available for these markers compared to *COI* (Weir and Cockerham 1984).

In contrast, the country-level genetic structure detected across all markers likely results from restricted gene flow at finer geographic scales (Urbanelli et al. 2000; Vazeille et al. 2001). These patterns are consistent with the hypothesis that limited dispersal capacity and geographic distance promote genetic differentiation (Zhong et al. 2013; Lucati et al. 2022). The presence of *A. albopictus* in both tropical and subtropical regions, along with genetic differences among populations, underscores a degree of population differentiation. Nevertheless, despite this genetic structuring, gene flow has also been detected among geographically distinct populations (Wilder-Smith and Gubler 2008).

Cluster analyses based on datasets comprising less than 50% of the available sequence data for the *COI* and *ND5* genes failed to recover a clear phylogenetic signal, resulting in branches with low statistical support and unresolved topological relationships. In contrast, clades derived from complete mitochondrial genome sequences were statistically well-supported. Although no clear geographic clustering was observed, the presence of diverse Asian haplotypes within the clades may suggest an invasion process originating from the native region toward different continents. This pattern is consistent with that observed in other global-scale studies using *COI* (Ruiling et al. 2018), *ND5* (Navarro et al. 2013), and complete mitochondrial genomes (Battaglia et al. 2022).

Previous phylogeographic studies of *A. albopictus* based on mitochondrial markers have reported varying levels of haplotype diversity. Ruiling et al. (2018) identified 76 *COI* haplotypes across 23 countries, while Navarro et al. (2013) recovered *16 ND5* haplotypes from 14 geographic locations. A more recent mitogenome-wide analysis by Battaglia et al. (2022) detected 47

haplotypes across 76 samples. In contrast, our study, which employed a global dataset compiled from publicly available genetic databases, revealed a substantially higher number of haplotypes: 255 for *COI* and 30 for *ND5*. This striking difference likely reflects the broader geographic and temporal scope of the publicly available data compared to earlier, more localized or smaller-scale studies.

Haplotype networks obtained for *COI*, *ND5*, and the mitochondrial genome suggest connectivity between the native region and all invaded areas. However, we did not observe geographic connection patterns among the invade areas. Despite this, connections between the Americas and Africa were consistently detected with all three markers. Other studies conducted with the same mitochondrial information from *COI*, *ND5*, and the mitochondrial genome have recovered a similar pattern, where the native area always shares genetic connections with invaded areas (Navarro et al. 2013; Ruiling et al. 2018; Battaglia et al. 2022). In *A. albopictus*, this pattern may be explained by the intercontinental dispersal of eggs or immature stages via passive maritime transport, primarily associated with the trade of used tires from Asia and, to a lesser extent, with the export of lucky bamboo—a well-documented phenomenon (Elbers et al. 2015; Ibañez-Justicia et al. 2020; Swan et al. 2022).

Currently, nuclear genetic markers for *A. albopictus*—including genomic data, SNP collections, and microsatellites —have enabled the reconstruction of phylogeographic patterns, colonization routes, and demographic inferences at local and regional scales (Vavassori, 2022; Pichler, 2019) and global scales (Cosme, 2024; Kotsakiozi, 2017; Goulbet, 2016). These findings have also been corroborated by mitochondrial gene and genome analyses (Battaglia et al. 2022). In our case, migration analyses using the three mitochondrial markers suggest that global mosquito populations conform to the panmixia hypothesis. This scenario implies that all populations behave as one, with high genetic exchange through random mating across all locations. Despite evaluating two scenarios that included major and minor maritime trade routes, these did not turn out to be the most plausible. We propose that this global panmixia is driven by human-assisted passive dispersal via maritime cargo transport, a pattern also documented in other invasive species such as *A. aegypti* (Gonçalves et al. 2012; Damal et al. 2013; Monsalve et al. 2021).

At the continental scale, cars have been identified as potential vectors for the dispersal of adult mosquitoes over smaller geographic ranges, such as within continents or between neighboring countries (Eritja et al. 2017). While the panmixia hypothesis has not been confirmed globally for other mosquito species, it has already been proposed at smaller geographic scales for other invasive species of the *Aedes* genus. For example, Monsalve et al. (2021) evaluated five migration hypotheses for *A. aegypti* in Colombia, including a total migration model, a panmixia model, and three stepping-stone models, using the mitochondrial genes *COI* and *ND4***,** as well as eight

microsatellites. In that study, it was found that the species' populations followed a panmixia hypothesis as a result of human-assisted transport, where geographical barriers did not limit gene flow between populations.

Our results are consistent with hypotheses previously evaluated for other mosquito species at smaller geographic scales, such as *A. aegypti* (Damal et al. 2013; Monsalve et al. 2021). However, we suggest that gene flow scenarios be evaluated on a global scale by incorporating additional genetic markers, such as SSRs and/or SNPs. As nuclear markers, these exhibit biparental inheritance, undergo recombination, and reflect more recent evolutionary events. In contrast, mitochondrial markers are strictly maternally inherited, lack recombination, and represent deeper evolutionary histories. Given these fundamental differences between nuclear and mitochondrial markers, evaluating the scenarios inferred in this study using nuclear genetic data could either support our current findings or provide alternative perspectives on the invasion dynamics of this species.The panmixia scenario suggests that all populations behave as a single unit, indicating a lack of genetic differentiation among them. Moreover, it implies high gene flow between populations at the global scale, although the number of migrants has not yet been quantified at this level. Therefore, we recommend evaluating this scenario using both nuclear and mitochondrial data. ABC results based on the three genetic markers suggest that Asia is the ancestral region from which *A. albopictus* was introduced into Europe, the Americas, and Africa. Yet, there is a discrepancy regarding how those populations from Asia spread among the invaded continents. Other studies have analyzed the demographic history of the tiger mosquito globally using microsatellites (Vega-Rúa et al. 2020), at the continental level using SNPs in Europe (Sherpa et al. 2019) and using *COI* in Oceania (Maynard et al. 2017). In all cases, Asia is consistently identified as the source region from which other parts of the world— including Europe and Oceania—were invaded.

Introduction events to the Indian Ocean islands (Africa) are supported by genetic evidence from the *COI* and *ND5* genes. However, the genetic information available for this population differs between the markers used. The *COI* gene, which included sequences from a greater number of localities within the population, suggests an introduction to Réunion Island, whereas the *ND5* gene contained sequences from only a single locality (Madagascar). This introduction event from Asia to the Indian Ocean islands has been supported by previous analyses using different markers (Paupy et al. 2001; Manni et al. 2017; Vega et al. 2020). In all cases, it is proposed that the Indian Ocean islands were the first area invaded by the mosquito, with this population resulting from an introduction event in the 18th century, possibly mediated by immigrants from Asia (Paupy et al. 2001).

Regarding the introduction event to Oceania, it is only supported by the *COI* gene, as there is no genetic information available for the other markers in that locality. Previous analyses using 13

SSRs and *COI* suggest that the populations that invaded Oceania are lineages from Asia, specifically from Indonesia (Cooper et al. 1994). It has been proposed that the introduction to this continent was mediated by maritime trade from Asia to Oceania through the Torres Strait (Beebe et al. 2013; Maynard et al. 2017).

The three markers propose an introduction of the mosquito to Europe in the late 1970s, which is consistent with its first record in Albania in 1979 (Adhami and Murati 1987). The introduction of the mosquito into Europe has been evaluated through different scenarios using ABC and employing different molecular markers (Manni et al. 2017; Sherpa et al. 2019; Vega-Rúa et al. 2020). All these studies suggest that *A. albopictus* invaded Europe—initially through Albania in the late 1970s—and concur that trade routes facilitated the introduction of multiple individuals into various countries across the continent from Asia (Manni et al. 2017; Sherpa et al. 2019; Vega-Rúa et al. 2020).

Regarding the introduction of the mosquito into North America, it was initially reported in 1985. For this scenario, there is evidence from mitogenomes (Battaglia et al. 2016), SNPs (Sherpa et al. 2019), and SSRs (Vega-Rúa et al. 2020) suggesting an invasion from Asia. Mitogenome results indicate a direct introduction from Japan, which could be explained by the presence of two primary maritime routes connecting China and Japan to the west coast of the USA. These maritime routes, along with international trade and the importation of used tires, facilitated multiple introductions of mosquito eggs and immature stages into North America (Hawley et al. 1987). Furthermore, secondary maritime routes also contribute—albeit to a lesser extent—to the spread of immature mosquitoes from Asia to North America, particularly through a secondary route linking Japan to the west coast of the United States (Rodrigue 2020).

The three mitochondrial markers suggest differing patterns regarding the invasion routes of *A. albopictus* into South America. The *COI* gene suggests a single invasion process from Asia, the *ND5* gene indicates a single introduction from the Indian Ocean islands, and the mitochondrial genome proposes multiple introductions from Asia and North America. To explain this incongruence, we propose a possible explanation: both partial mitochondrial genes and the complete mitochondrial genome support evidence of multiple introduction events into South America, as previously reported in the literature (Vega-Rúa et al. 2020). These introductions could be explained by distinct maritime trade routes linking various regions of the world to South America.

The three markers suggest that African populations were directly introduced from Asia and were established in the 1990s. These results could be explained by secondary maritime trade routes connecting Southeast Asia and South Africa, as they constitute one of the most transited routes globally (Troch et al. 2021 These trade routes may have facilitated the introduction of *A. albopictus*

into Africa from Asia, as proposed by several authors since 1991, including reports from South Africa (Cornel and Hunt 1991), Mali (Diallo et al. 2010), and the Central African Republic (Müller et al. 2016). Nonetheless, our results are incongruent with what was found in previous analyses using SSRs, as they suggest a founder event from populations in South America (Brazil) to Africa (Congo) (Vega-Rúa et al. 2020). We propose two possible explanations for this inconsistency: (i) the number of sampling locations differed between the two studies, which may have led to the recovery of distinct invasion scenarios; and (ii) nuclear genetic markers such as SSRs and mitochondrial markers may reflect different demographic histories. In either case, we recommend expanding the use of nuclear markers to better explain both scenarios.

CONCLUSIONS

This study provides a valuable contribution to our understanding of the global genetic diversity, population structure, gene flow, invasion dynamics, and demographic history of the tiger mosquito. It highlights the high genetic diversity observed in Asia, supporting established global phylogeographic patterns and colonization routes. The findings indicate that meaningful insights into the colonization processes and demographic history of medically important invasive species can be obtained from a limited number of mitochondrial genetic markers, despite their lower resolution compared to multi-locus nuclear markers with higher levels of polymorphism. Our results support the hypothesis of high genetic diversity in *A. albopictus* within its native region of Asia. At the continental scale, there is no clear population structuring, suggesting extensive gene flow between populations, likely driven by global maritime connectivity. Genetic links were detected between the native range and all invaded regions across continents. Results from all mitochondrial markers are consistent with a panmictic population structure, characterized by random mating and high gene flow among populations. This pattern is likely promoted by human-assisted dispersal, which helps maintain genetic diversity on a global scale. These findings highlight the critical role of human transportation in both the spread and genetic homogenization of this invasive species. Increased attention from vector control programs is needed in regions heavily involved in international trade, particularly those associated with the movement of goods capable of harboring immature mosquito stages. Bayesian analyses support Southeast Asia as the ancestral region, from which the species first invaded the Indian Ocean islands (Africa) as early as the 18th century, and other continents over the past 50 years. This study underscores how the expansion of global commerce facilitates biological invasions—such as that of the tiger mosquito—through passive, human-mediated intercontinental transport.

Acknowledgments: The authors express their gratitude to the University of Quindío, particularly to the Research Vice-Rectory, for funding this work under Project 1168.

Authors' contributions: JCLS and CEFE conducted the information search and analysis processing. BSVM contributed to the analytical aspect regarding the use of R and coalescence. OAAO conceived the study, provided guidance, and assisted in manuscript review. All authors contributed equally to the writing of the manuscript.

Competing interests: The authors declare no competing interests

Availability of data and materials:

Consent for publication:

Ethics approval consent to participate:

REFERENCES

Adhami J, Murati N. 1987. The presence of the mosquito *Aedes albopictus* in Albania. *Mjekësore* **1:**13–16.

Aguirre-Obando OA, Navarro-Silva MA. 2017. How much is known about the genetic diversity of the Asian tiger mosquito? A systematic review. Revista de La Universidad Industrial de Santander. Salud **49:**422–437. doi:10.18273/revsal.v49n3-2017001.

Anoopkumar AN, Puthur S, Varghese P, Rebello S, Aneesh EM. 2017. Life cycle, bio-ecology and DNA barcoding of mosquitoes *Aedes aegypti* (Linnaeus) and *Aedes albopictus* (Skuse). Journal of Communicable Diseases **49:**32–41. doi:10.24321/0019.5138.201719.

Athrey G, Hodges TK, Reddy MR, Overgaard HJ, Matias A et al. 2012. The Effective Population Size of Malaria Mosquitoes: Large Impact of Vector Control. PLoS Genetics **8:**e1003097. doi:10.1371/journal.pgen.1003097.

Battaglia V, Agostini V, Moroni E, Colombo G, Lombardo G et al. 2022. The worldwide spread of *Aedes albopictus*: New insights from mitogenomes. Frontiers in Genetics **13:**931163. doi:10.3389/fgene.2022.931163.

Battaglia V, Gabrieli P, Brandini S, Capodiferro MR, Javier PA et al. 2016. The worldwide spread of the tiger mosquito as revealed by mitogenome haplogroup diversity. Frontiers in Genetics **7:**208. doi:10.3389/fgene.2016.00208.

Baele G, Suchard M, Rambaut A, Lemey P. 2017. Emerging Concepts of Data Integration in Pathogen Phylodynamics. Syst Biol **66:**e47–e65. doi:10.1093/sysbio/syw054.

Becker N, Pluskota B, Kaiser A, Schaffner F. 2012. Exotic mosquitoes conquer the world. *In*: Mehlhorn H. (eds) Arthropods as Vectors of Emerging Diseases. Parasitology Research Monographs, vol 3. Springer, Berlin, Heidelberg. doi:10.1007/978-3-642-28842-5_2.

Beebe N, Ambrose L, Hill L, Davis J, Hapgood G et al. 2013. Tracing the tiger: Population genetics provides valuable insights into the *Aedes* (*Stegomyia*) *albopictus* invasion of the Australasian region. Plos Negleted Tropical Diseases **7:**e2361. doi:10.1371/journal.pntd.0002361.

Beerli P, Mashayekhi S, Sadeghi M, Khodaei M, Shaw K. 2019. Population Genetic Inference With MIGRATE. Current Protocols in Bioinformatics **68:**e87. doi:10.1002/cpbi.87.

Beerli P, Palczewski M. 2010. Unified Framework to Evaluate Panmixia and Migration Direction Among Multiple Sampling Locations. Genetics **185:**313–326. doi:10.1534/GENETICS.109.112532.

Benelli G, Wilke ABB, Beier JC. 2020. *Aedes albopictus* (Asian Tiger Mosquito). Trends Parasitol **36:**942–943. doi:10.1016/j.pt.2020.01.001.

Birungi J, Munstermann L. 2002. Genetic structure of *Aedes albopictus* (Diptera: Culicidae) populations based on Mitochondrial ND5 sequences: evidence for an independent invasion into Brazil and United States. Genetics **95:**125–132. doi:10.1603/0013-8746(2002)095[0125:GSOAAD]2.0.CO;2.

Boissin E, Hurley B, Wingfield MJ, Vasaitis R, Stenlid J et al. 2012. Retracing the routes of introduction of invasive species: The case of the *Sirex noctilio* woodwasp. Mol Ecol **21:**5728–5744. doi:10.1111/mec.12065.

Bonizzoni M, Gasperi G, Chen X, James AA. 2013. The invasive mosquito species *Aedes albopictus*: Current knowledge and future perspectives. Trends Parasitol **29:**460–468. doi:10.1016/j.pt.2013.07.003.

Carlton J. 1987. Patterns of transoceanic marine biological invasions in the Pacific Ocean. B Mar Sci **41:**452–465.

Carter M, Smith M, Harrison R. 2010. Genetic analyses of the Asian longhorned beetle (Coleoptera, Cerambycidae, *Anoplophora glabripennis*), in North America, Europe and Asia. Biol Invasions **12:**1165–1182. doi:10.1007/s10530-009-9538-9.

Comeault AA, Wang J, Tittes S, Isbell K, Ingley S, Hurlbert AH, Matute DR. 2020. Genetic diversity and thermal performance in invasive and native populations of African Fig Flies. Mol Biol Evol **37:**1893–1906. doi:10.1093/molbev/msaa050.

Cooper RD, Waterson DGE, Kupo M, Sweeney AW. 1994. *Aedes albopictus* (Skuse) (Diptera: Culicidae) in the Western Province of Papua New Guinea and the threat of its introduction to Australia. Aust J Entomol **33:**115–116. doi:10.1111/j.1440-6055.1994.tb00933.x.

Cornuet JM, Pudlo P, Veyssier J, Dehne-Garcia A, Gautier M et al. 2014. DIYABC v2.0: a software to make approximate Bayesian computation inferences about population history using single nucleotide polymorphism, DNA sequence and microsatellite data. Bioinformatics **30:**1187–1189. doi:10.1093/BIOINFORMATICS/BTT763.

Cosme LV, Corley M, Johnson T, Severson DW, Yan G et al. 2024. A genotyping array for the globally invasive vector mosquito, *Aedes albopictus*. Parasites Vectors **17:**106. doi:10.1186/s13071-024-06158-z.

Damal K, Murrell E, Juliano S, Conn J, Loew S. 2013. Phylogeography of *Aedes aegypti* (Yellow Fever Mosquito) in South Florida: mtDNA Evidence for Human-Aided Dispersal. Am J Trop Med Hyg **89:**482–488. doi:10.4269/ajtmh.13-0102.

Ditter RE, Campos M, Pinto J, Cornel AJ, Rompão H, Lanzaro GC. 2022. Mitogenome Analyses Reveal Limited Introduction of *Anopheles coluzzii* Into the Central African Islands of São Tomé and Príncipe. Frontiers Tropical Diseases **3:**855272. doi:10.3389/fitd.2022.855272.

Elbers ARW, Koenraadt CJ, Meiswinkel R. 2015. Mosquitoes and Culicoides biting midges: vector range and the influence of climate change. Rev Sci Tech **34:**123–137. doi:10.20506/rst.34.1.2349

Eritja R, Palmer J, Roiz D, Sanpera-Calbet I, Bartumeus F. 2017. Direct evidence of adult *Aedes albopictus* dispersal by Car. Nature **7:**14399. doi:10.1038/s41598-017-12652-5.

Estoup A, Ravigné V, Hufbauer R, Vitalis R, Gautier M, Facon B. 2016. Is There A Genetic Paradox of Biological Invasion? Ann Rev Ecol, Evol, S **47:**51–72. doi:10.1146/annurev-ecolsys-121415–032116.

Fikrig K, Harrington LC. 2021. Understanding and interpreting mosquito blood feeding studies: the case of *Aedes albopictus*. Trends Parasitol **37:**959–975. doi:10.1016/j.pt.2021.07.013.

Fischer ML, Hochkirch A, Heddergott M, Schulze C, Anheyer-Behmenburg HE et al. 2015. Historical invasion records can be misleading: Genetic evidence for multiple introductions of invasive raccoons (*Procyon lotor*) in Germany. PLoS ONE **10:**e0125441. doi:10.1371/journal.pone.0125441.

Fontaine MC, Labbé F, Dussert Y, Delière L, Richart-Cervera S, Giraud T, Delmotte F. 2021. Europe as a bridgehead in the worldwide invasion history of grapevine downy mildew, *Plasmopara viticola*. Curr Biol **31:**2155–2166.e4. doi:10.1016/j.cub.2021.03.009.

Frost S, Pybus O, Cog J, Viboud C, Bonhoeffer S, Bedford T. 2015. Eight challenges in phylodynamic inference. Epidemics **10:**88–92. doi:10.1016/j.epidem.2014.09.001.

Gonçalves A, Cunha I, Santos W, Luz S, Ribolla P, Abad-Franch F. 2012. Gene flow networks among American *Aedes aegypti* populations. Evol Appl **5:**664–676. doi:10.1111/j.1752-4571.2012.00244.x.

Gotzek D, Axen HJ, Suarez AV, Helms Cahan S, Shoemaker D. 2015. Global invasion history of the tropical fire ant: A stowaway on the first global trade routes. Mol Ecol **24:**374–388. doi:10.1111/mec.13040.

Hasan AU, Suguri S, Ahmed SMU, Fujimoto C, Harada M., Rahman SM, Zaman R, U, Kakehi Y. 2009. Molecular phylogeography of *Culex quinquefasciatus* mosquitoes in central Bangladesh. Acta Tropica **112:**106–114. doi:10.1016/j.actatropica.2009.07.005.

Hawley W, Reiter P, Copeland R, Pumpuni C, Craig R Jr. 1987. *Aedes albopictus* in North America: Probable introduction in used tires from Northern Asia. Science **236:**1114–1116. doi:10.1126/science.3576225

Hudson J, Bourne S, Seebens H, Chapman M, Rius M. 2022. The reconstruction of invasion histories with genomic data in light of differing levels of anthropogenic transport. Philosophical transations B **377:**20210023. doi:10.1098/rstb.2021.0023.

Ibáñez-Justicia A. 2020. Routess for introduction and dispersal of invasive *Aedes* mosquito species in Europe: a review. Journal of the European Mosquito Control Association **38:**1–10.

Ibáñez-Justicia A, Vossenberg B, van de Warbroek T, Teekema S, Jacobs F et al. 2022. Tracking Asian tiger mosquito introductions in the Netherlands using Nextstrain. Journal of the European Mosquito Control Association **40:**11–21. doi:10.52004/JEMCA2021.0006.

Katoh K, Rozewicki J, Yamada KD. 2018. MAFFT online service: Multiple sequence alignment, interactive sequence choice and visualization. Briefings in Bioinformatics **20:**1160–1166. doi:10.1093/bib/bbx108.

Kotsakiozi P, Richardson JB, Pichler V, Favia G, Martins AJ et al. 2017. Population genomics of the Asian tiger mosquito, *Aedes albopictus*: insights into the recent worldwide invasion. Ecol and Evol **7:**10143–10157. doi:10.1002/ece3.3514.

Kraemer MUG, Sinka ME, Duda KA, Mylne A, Shearer FM et al. 2015. The global compendium of *Aedes aegypti* and *Ae. albopictus* occurrence. Scientific Data **2:**1–8. doi:10.1038/sdata.2015.35.

Láruson A, Reed F. 2021. Population Genetics with R (1st ed.). OXFORD UNIVERSITY PRESS.

Latreille AC, Milesi P, Magalon H, Mavingui P, Atyame CM. 2019. High genetic diversity but no geographical structure of *Aedes albopictus* populations in Reúnion Island. Parasit Vectors **12:**597. doi:10.1186/s13071-019-3840-x.

Lucati F, Delacour S, Palmer JRB, Caner J, Oltra A et al. 2022. Multiple invasions, *Wolbachia* and human-aided transport drive the genetic variability of *Aedes albopictus* in the Iberian Peninsula. Scientific Reports **12:**20682. doi:10.1038/s41598-022-24963-3.

Magalhaes T, Robison A, Young M, Black W, Foy B et al. 2018. Sequential Infection of *Aedes aegypti* Mosquitoes with Chikungunya Virus and Zika Virus Enhances Early Zika Virus Transmission. Insects **9:**177. doi:10.3390/insects9040177.

Magee D, Suchard M, Scotch M. 2017. Bayesian phylogeography of influenza A/H3N2 for the 2014-15 season in the United States using three frameworks of ancestral state reconstruction. Plos Comput Biol **13:**e1005389. doi:10.1371/journal.pcbi.1005389.

Mallez S, Castagnone C, Lombaert E, Castagnone-Sereno P, Guillemaud T. 2021. Inference of the worldwide invasion routes of the pinewood nematode *Bursaphelenchus xylophilus* using approximate Bayesian computation analysis. Peer Community Journal **1:**e56. doi:10.24072/pcjournal.64.

Manni M, Guglielmino CR, Scolari F, Vega-Rúa A, Failloux AB et al. 2017. Genetic evidence for a worldwide chaotic dispersion pattern of the arbovirus vector, *Aedes albopictus*. PLoS Neglect Trop D **11:**1–22. doi:10.1371/journal.pntd.0005332.

Maynard AJ, Ambrose L, Cooper RD, Chow WK, Davis JB et al. 2017. Tiger on the prowl: Invasion history and spatio-temporal genetic structure of the Asian tiger mosquito *Aedes albopictus* (Skuse 1894) in the Indo-Pacific. PLoS Neglect Trop D **11:**1–27. doi:10.1371/journal.pntd.0005546.

Monsalve Y, Triana-Chávez O, Gomez-Palacio A. 2021. Population structure and ancestry prediction of *Aedes aegypti* (Diptera: Culicidae) supports a single African origin of Colombian populations. Mem Inst Oswaldo **116:**e200441. doi:10.1590/0074-02760200441.

Moore M, Sylla M, Goss L, Burugu MW, Sang R et al. 2013. Dual African Origins of Global *Aedes aegypti* s.l. Populations Revealed by Mitochondrial DNA. PLoS Neglect Trop D **7:**e2175. doi:10.1371/journal.pntd.0002175.

Morgan K, O'Loughlin SM, Chen B, Linton YM, Thongwat D et al. 2011. Comparative phylogeography reveals a shared impact of pleistocene environmental change in shaping genetic diversity within nine *Anopheles* mosquito species across the Indo-Burma biodiversity hotspot. Mol Ecol **20(21):**4533–4549. doi:10.1111/j.1365-294X.2011.05268.x.

Nadel RL, Slippers B, Scholes MC, Lawson SA, Noack AE et al. 2010. DNA bar-coding reveals source and patterns of *Thaumastocoris peregrinus* invasions in South Africa and South America. Biol Invasions **12:**1067–1077. doi:10.1007/s10530-009-9524-2.

Näslund J, Ahlm C, Islam K, Evander M, Bucht G, Lwande OW. 2021. Emerging Mosquito-Borne Viruses Linked to *Aedes aegypti* and *Aedes albopictus*: Global Status and Preventive Strategies. Vector-Borne Zoonot **21:**731–746. doi:10.1089/vbz.2020.2762.

Navarro J, Quintero L, Zorrilla A, González R. 2013. Molecular Tracing with Mitochondrial ND5 of the Invasive Mosquito *Aedes* (Stegomyia) *albopictus* (Skuse) in Northern South America. Journal of Entomology and Zoology Studies **1:**32–39.

Neophytou C. 2013. Bayesian clustering analyses for genetic assignment and study of hybridization in oaks: effects of asymmetric phylogenies and asymmetric sampling schemes. Tree Genetics & Genomes **10:**273–285. doi:10.1007/s11295-013-0680-2.

Oliveira S, Rocha J, Sousa CA, Capinha C. 2021. Wide and increasing suitability for *Aedes albopictus* in Europe is congruent across distribution models. Sci Rep **11:**1–9. doi:10.1038/s41598-021-89096-5.

Paradis E. 2010. Pegas: An R package for population genetics with an integrated-modular approach. Bioinformatics **26:**419–420. doi:10.1093/bioinformatics/btp696.

Paupy C, Delatte H, Bagny L, Corbel V, Fontenille D. 2009. *Aedes albopictus*, an arbovirus vector: From the darkness to the light. Microbes Infect **11:**1177–1185. doi:10.1016/j.micinf.2009.05.005.

Peretolchina T, Pavan MG, Corrêa-Antônio J, Gurgel-Gonçalves R, Lima MM et al. 2018. Phylogeography and demographic history of the Chagas disease vector *Rhodnius nasutus* (Hemiptera: Reduviidae) in the Brazilian Caatinga biome. PLoS Neglect Trop D **12:**e0006731. doi:10.1371/journal.pntd.0006731.

Pichler V, Kotsakiozi P, Caputo B, Serini P, Caccone A, Della Torre A. 2019. Complex interplay of evolutionary forces shaping population genomic structure of invasive *Aedes albopictus* in southern Europe. PLoS Neglect Trop D **13:**e0007554. doi:10.1371/journal.pntd.0007554.

Porretta D, Mastrantonio V, Bellini R, Somboon P, Urbanelli S. 2012. Glacial History of a Modern Invader: Phylogeography and Species Distribution Modelling of the Asian Tiger Mosquito *Aedes albopictus*. PLoS ONE **7:**e44515. doi:10.1371/journal.pone.0044515.

Posada D. 2008. jModelTest: Phylogenetic Model Averaging. Mol Biol Evol **25:**1253–1256. doi:10.1093/MOLBEV/MSN083.

Puechmaille S. 2016. The program STRUCTURE does not reliably recover the correct population structure when sampling is uneven: subsampling and new estimators alleviate the problem. Mol Ecol Resour **16:**608–627. doi:10.1111/1755-0998.12512.

QGIS.org. 2024. QGIS Geographic Information System. QGIS Association. Available at: http://www.qgis.org.

Rasmussen D. Grünwald N. 2021. Phylogeographic approaches to characterize the emergence of plant pathogens. Phytopathology **111:**68–77. doi:10.1094/PHYTO-07-20-0319-FI.

Rodrigue JP. 2020. The Geography of Transport Systems. Available at: https://transportgeography.org/.

Ruiling Z, Tongkai L, Dezhen M, Zhong Z. 2018. Genetic characters of the globally spread tiger mosquito, *Aedes albopictus* (Diptera, Culicidae): implications from mitochondrial gene *COI*. J Vector Ecol **43:**89–97. doi:10.1111/jvec.12287.

Sherpa S, Rioux D, Pougnet-Lagarde C, Després L. 2018. Genetic diversity and distribution differ between long-established and recently introduced populations in the invasive mosquito *Aedes albopictus*. Infection, Genetics and Evolution **58:**145–156. doi:10.1016/j.meegid.2017.12.018.

Sherpa S, Blum MGB, Capblancq T, Cumer T, Rioux D, Després L. 2019. Unravelling the invasion history of the Asian tiger mosquito in Europe. Mol Ecol **28:**2360–2377. doi:10.1111/mec.15071.

Shin J, Rahman MM, Kim J, Marcombe S, Jung J. 2023. Genetic Diversity of Dengue Vector *Aedes albopictus* Collected from South Korea, Japan, and Laos. Insects **14:**297. doi:10.3390/insects14030297.

Suesdek L. 2019. Microevolution of medically important mosquitoes–A review. Acta Tropica **191:**162–171. doi:10.1016/j.actatropica.2018.12.013.

Swan T, Russell TL, Staunton KM, Field MA, Ritchie SA, Burkot TR. 2022. A literature review of dispersal routess of *Aedes albopictus* across different spatial scales: implications for vector surveillance. Parasites Vectors **15:**303. doi:10.1186/s13071-022-05413-5.

Tajima F. 1989. Statistical method for testing the neutral mutation hypothesis by DNA polymorphism. Genetics **123:**585–595. doi:10.1093/genetics/123.3.585.

Tajima F, Misawa K, Innan H. 1998. The amount and pattern of DNA polymorphism under the neutral mutation hypothesis. Genetica **102:**103–107. doi:10.1023/A:1017011631572.

Templeton AR, Crandall KA, Sing CF. 1992. A cladistic analysis of phenotypic associations with haplotypes inferred from restriction endonuclease mapping and DNA sequence data. III. Cladogram estimation. Genetics **132:**619–633. doi:10.1093/genetics/132.2.619.

Troch C, Terblanche L, Henning H. 2021. Modelling and measurement of low-frequency surge motion associated with extreme storm conditions in the Port of Cape Town. Applied Ocean Research **106:**102452. doi:10.1016/j.apor.2020.102452.

Urbanelli S, Bellinià R, Carrierià M, Sallicandro P, Celli G. 2000. Population structure of *Aedes albopictus* (Skuse): the mosquito which is colonizing Mediterranean countries. Heredity **84:**331–337. doi:10.1046/j.1365-2540.2000.00676.x.

Vavassori L, Honnen A C, Saarman N, Caccone A, Müller P. 2022. Multiple introductions and overwintering shape the progressive invasion of *Aedes albopictus* beyond the Alps. Ecol Evol **12:**e9138. doi:10.1002/ece3.9138.

Vazeille M, Mousson L, Rakatoarivony I, Villeret R, Rodhain F, Duchemin JB, Failloux AB. 2001. Population genetic structure and competence as a vector for dengue type 2 virus of *Aedes aegypti* and *Aedes albopictus* from Madagascar. ASTMH **65:**491–497. doi:10.4269/ajtmh.2001.65.491.

Vega-Rúa A, Marconcini M, Madec Y, Manni M, Carraretto D et al. 2020. Vector competence of *Aedes albopictus* populations for chikungunya virus is shaped by their demographic history. Communications Biology **3:**25–28. doi:10.1038/s42003-020-1046-6.

Waldbieser GC, Lelania Bilodeau A, Nonneman DJ. 2003. Complete sequence and characterization of the channel catfish mitochondrial genome. DNA Sequence **14:**265–277. doi:10.1080/1042517031000149057.

Waldock J, Chandra NL, Lelieveld J, Proestos Y, Michael E, Christophides G, Parham PE. 2013. The role of environmental variables on *Aedes albopictus* biology and chikungunya epidemiology. Pathog Glob Health **107:**224. doi:10.1179/2047773213Y.0000000100.

Wang J. 2017. The computer program structure for assigning individuals to populations: easy to use but easier to misuse. Mol Ecol Res **17:**981–990. doi:10.1111/1755-0998.12650.

Weir BS, Cockerham CC. 1984. Estimating *F*-Statistics for the Analysis of Population Structure. Evolution **38:**1358. doi:10.2307/2408641.

Wibowo A. 2021. Phylogeography and Proline amino acid usage of Asian tiger mosquito *Aedes albopictus* (Skuse 1894) populations along landscape gradients in Indonesia. BioRvix. doi:10.1101/2021.03.14.435316.

Wilder-Smith A, Gubler DJ. 2008. Geographic expansion of dengue: the impact of international travel. Med Clin N Am **92:**1377–1390. doi:10.1016/j.mcna.2008.07.002.

Supplementary materials

Table S1. List of mitochondrial gene names and their abbreviations. Adapted from Waldbieser et al. (2003). (download)

Table S2. Updated first record of *Aedes albopictus* worldwide. (download)

Table S3. Global-, continental-, and country-level analyses for the *COI*, *ND5*, and mitochondrial genome markers of the tiger mosquito. Results include haplotype diversity (Hd), nucleotide diversity (π), and neutrality tests. (download)

Table S4. Effective sample size values for the Bayesian analyses of the *COI*, *ND5*, and mitochondrial genome datasets. (download)

Table S5. Results of the demographic history scenarios evaluated for the tiger mosquito, including the groups of scenarios analyzed, descriptions of their directionality, posterior probabilities, and confidence test outcomes for each scenario. (download)